Safety Science 50 (2012) 986–994

Contents lists available at SciVerse ScienceDirect

Safety Science

journal homepage: www.elsevier.com/locate/ssci

# Development of new footwear sole surface pattern for prevention of slip-related falls

Takeshi Yamaguchi [a,*], Tomoki Umetsu [a], Yusuke Ishizuka [a], Kenichi Kasuga [b], Takayuki Ito [b], Satoru Ishizawa [b], Kazuo Hokkirigawa [a]

[a] Graduate School of Engineering, Tohoku University, 6-6-01 Aramaki-Aza-Aoba, Aoba-ku, Sendai, Miyagi 980-8579, Japan
[b] Kohshin Rubber Co., Ltd., 2-1-11 Kawaramachi, Wakabayashi-ku, Sendai, Miyagi 984-0816, Japan

ARTICLE INFO

*Article history:*
Received 26 February 2010
Received in revised form 2 July 2011
Accepted 15 December 2011
Available online 20 January 2012

*Keywords:*
Coefficient of friction
Fall
Footwear
Slip
Rubber

ABSTRACT

In this study, a new rubber surface pattern for a footwear sole was developed to prevent slip-related falls. This pattern shows a high static coefficient of friction (SCOF) and a high dynamic coefficient of friction (DCOF) when sliding against a liquid contaminated surface. A hybrid rubber block, in which a rubber block with a rough surface (Ra = 30.4 μm) was sandwiched between two rubber blocks with smooth surfaces (Ra = 0.98 μm), was prepared. The ratio of the rough surface area to the whole rubber block surface area *r* was 0%, 30%, 50%, 80%, and 100%. The coefficient of friction of the rubber blocks was measured when sliding against a stainless steel plate with Ra of 0.09 μm contaminated with a 90% aqueous solution of glycerol. While the SCOF increased with an increase of the rough surface area ratio *r*, the DCOF during steady-state sliding decreased with an increase of the rough surface area ratio *r*. The rough surface area ratio of 50% achieved a SCOF value around 0.5 or more and a DCOF value greater than 0.5. Furthermore, the difference in the value of the SCOF and DCOF was the smallest for the rubber block with *r* of 50%. The results indicated that the rubber block with *r* of 50% would be applicable to a footwear sole surface pattern to prevent slip and fall accidents on contaminated surfaces.



## 1. Introduction

The number of slip and fall incidents in occupational accidents has been increasing in Japan as well as in other industrialized countries. (Ministry of Health, Labor and Welfare, 2006; Courtney et al., 2001; Courtney and Webster, 2001). Most slip and fall accidents in the workplace occur on liquid contaminated floor surfaces (Strandberg, 1985; Proctor and Coleman, 1988; Grönqvist, 1995; Leclercq et al., 1995; Manning and Jones, 2001). Such smooth floor surface is slippery when contaminated with water or oil due to the formation of a fluid film in the contact interface between the footwear sole and the floor. Thus, a footwear sole pattern with a high slip-resistance, even on such slippery surface, is required to prevent slip-related falls.

The coefficient of friction is often used for the evaluation of the slip resistance of a footwear sole. There have been controversies in selecting either static friction or dynamic friction as the critical frictional parameter at the contact interface between the footwear sole and the floor for the prevention of slip-related falls (Ekkubus and Killey, 1973; Tisserand, 1985; Pilla, 2003; Yamaguchi and Hokkirigawa, 2008). As Perkins (1978) pointed out, slip velocity and slip distance, which both have a strong correlation with a fall due to induced slip, increase with the difference of the values of static coefficient of friction (SCOF) and dynamic coefficient of friction (DCOF). In particular, if the SCOF is high but the DCOF was very low, slippage may not be stopped when the required coefficient of friction (RCOF) reaches the SCOF, resulting in slip initiation. On the other hand, if the SCOF is small enough for slip to occur but the DCOF is high, slippage stops and a fall will be avoided. Therefore, it has recently been considered that the DCOF is a more relevant measurement from slip biomechanics studies (Strandberg and Lanshammar, 1981; Perkins and Wilson, 1983; Strandberg, 1983; Grönqvist et al., 1989), and it is insufficient to evaluate the slip-resistance of shoe soles and floors only with the value of SCOF. However, if we have a shoe sole pattern which provides sufficiently high SCOF and DCOF, it would be safer because it helps to prevent slip initiation and to stop slip even if it occurs. The safe limit of DCOF for walking on level floor was suggested to be 0.20–0.40 by various studies (Grönqvist et al., 1989, 2003; Redfern and Bidanda, 1994; Strandberg, 1983). Fong et al. (2009) reported that humans walk carefully to avoid slipping when the DCOF drops below 0.41. Grönqvist et al. (2003) suggested that the limit for preventing a slip was in the range 0.3–0.35, and if the DCOF was below this limit, a person would change their gait to adapt to the slippery surface. Nagata et al. (2009) also suggested that the fall risk due

* Corresponding author. Tel.: +81 22 795 6897.
*E-mail address:* yamatake@gdl.mech.tohoku.ac.jp (T. Yamaguchi).

0925-7535/$ - see front matter © 2011 Elsevier Ltd. All rights reserved.
doi:10.1016/j.ssci.2011.12.017

to induced slip increased when the coefficient of friction was below 0.4 based on a ramp test. Therefore, values of SCOF and DCOF greater than 0.4 would be required for the shoe sole/floor interface. However, too high friction could introduce tripping, and it is difficult to determine the upper limits of DCOF and SCOF to prevent this occurring.

The velocity of the slipping foot, which is also believed to be one of the determinants of whether an induced slip will result in the fall or the postural recovery (Perkins, 1978; Perkins and Wilson, 1983; James, 1990), is a function of the difference between the values of SCOF and DCOF (Tisserand, 1985). Thus, reduction in the difference between these values would also be one of the critical frictional properties between the footwear sole and the floor.

According to Bowen and Tabor (1950), friction force is a sum of an adhesive friction term ($F_{adh}$) and a deformation friction term ($F_{def}$), as given by

$$F = F_{adh} + F_{def} \quad (1)$$

Adhesive friction results from the contact and subsequent shearing of individual surface asperities; and the deformation component is due to the ploughing or other forms of deformation caused by the harder surface on the softer surface. When a rubber slides on a smooth harder surface, the ploughing effect can be neglected. Hence the adhesive friction is directly proportional to the real area of contact and is given by

$$F = \tau A_r \quad (2)$$

where $\tau$ is the interfacial shear strength of the contact and $A_r$ is the real area of contact.

The elastic modulus of rubber, usually used as footwear sole material, is low compared to other engineering materials. Hence, a high real area of contact between mating surfaces provides high values of static and dynamic friction under dry conditions. However, when sliding against a smooth surface contaminated with water or oil, a fluid film may be formed at the contact interface. The interfacial shear strength is determined by the fluid film, which results in low values of static and dynamic friction. Therefore, increasing the amount of contact area between the rubber and the mating surface by removing the fluid film is important to increase the coefficient of friction under lubricated conditions.

The slip resistance, i.e. coefficient of friction, of shoe soles with various tread pattern (macroscopic pattern) and surface roughness (microscopic pattern) characteristics has been measured on contaminated floors (Grönqvist, 1995; Grönqvist et al., 1999; Wilson, 1990; Chang et al., 2001a; Li and Chen, 2004, 2005). These studies indicated that the surface roughness and tread pattern of the shoe sole are helpful for liquid drainage to increase the coefficient of friction. Hence the surface pattern design of a rubber sole, including tread pattern and surface roughness, is of great importance in improving slip-resistance. However, adequate design criteria (guidelines) for a shoe sole pattern with sufficient slip resistance on contaminated surfaces have not been fully understood. Therefore, the surface pattern design of the footwear sole required to increase SCOF and DCOF on contaminated surfaces is unclear.

In this study, a new rubber surface pattern for footwear soles using a hybrid rubber block combining smooth and rough surfaces, which showed sufficiently high SCOF and DCOF when slid against a liquid contaminated surface, was developed. The mechanisms of the increased SCOF and DCOF of the hybrid rubber block were also investigated based on the contact area measurement between the rubber block surface and the counterpart material surface by use of total reflection of light.

## 2. Methods

### 2.1. Sample preparation

NBR (acrylonitrile butadiene rubber) was formed into a rectangular block geometry (25 mm × 25 mm × 5 mm) using two kinds of metallic molds with different surface roughness. The tensile strength of the NBR was 9.52 MPa, the elongation was 875%, the 300% modulus was 1.12 MPa, and the shore hardness (*A*/15) was 45. The surface roughness Ra of each rubber block was 0.98 μm (smooth surface) or 30.4 μm (rough surface). The hybrid rubber blocks, in which a rubber block with a rough surface was sandwiched between rubber blocks of the same size but a smooth surface, were prepared as shown in Fig. 1a and b. The rubber blocks were adhered with a modified silicon adhesive. The rough surface area ratio *r* was defined as following formula;

$$r = \frac{a}{25} \times 100\ [\%] \quad (3)$$

where *a* is length of the rubber block with a rough surface in the sliding direction (mm). Rubber blocks with rough surface area ratio *r* values of 0%, 30%, 50%, 80%, and 100% were prepared. Fig. 1c shows the topography of the rubber blocks (surface profile curves), which was measured with a contact type stylus profiler (Poon and Bhushan, 1995). The stylus was loaded on the surface to be measured and then moved across the surface along the sliding direction of the friction test at a constant velocity, to obtain surface height variation.

### 2.2. Experimental setup

In this study, the following two kinds of friction test were carried out using a reciprocating linear sliding type tribo-meter (SHINTO Scientific Co., Ltd.). The friction tests of the rubber blocks were conducted on a polished stainless steel plate (JIS SU304) and a polished glass plate. Stainless steel with smooth surface is commonly used as a floor material in food processing plants, where sanitary control is valued, from the viewpoint of ease of cleaning. Therefore, a polished stainless steel plate was used as one of the mating materials. On the other hand, the friction tests on a polished glass plate were conducted in order to measure the contact area between the rubber block sample and the mating surface and discuss its effect on the coefficients of friction by using the total reflection of light.

#### 2.2.1. Friction test sliding against a polished stainless steel plate

Fig. 2 shows a schematic diagram of the experimental setup for the friction tests between the rubber block and the polished stainless steel plate. The rubber block sample glued on the base rubber block (the same NBR, 30 mm × 30 mm × 20 mm) was affixed on the sample holder. The rubber block was slid against the stainless steel plate (500 mm × 60 mm × 1 mm) with surface roughness Ra of 0.09 μm mounted on a linear motion stage. The linear motion stage was driven by a servo-motor through a ball screw. A normal load was applied by a 56.6 N dead weight. Friction force was measured with a push–pull type force gauge, and the friction force data were recorded by a digital data logger. The coefficient of friction was calculated by dividing the friction force by the normal load. The SCOF was the coefficient of friction at the time when a macroscopic slip occurred between rubber block and the mating stainless steel plate, which was determined by observation of the contact interface viewed from the side with a high speed camera (MotionPro X3, IDT Japan, Inc.). The steady-state DCOF was taken as the mean value of the coefficient of friction while the stage velocity (sliding velocity) was constant.

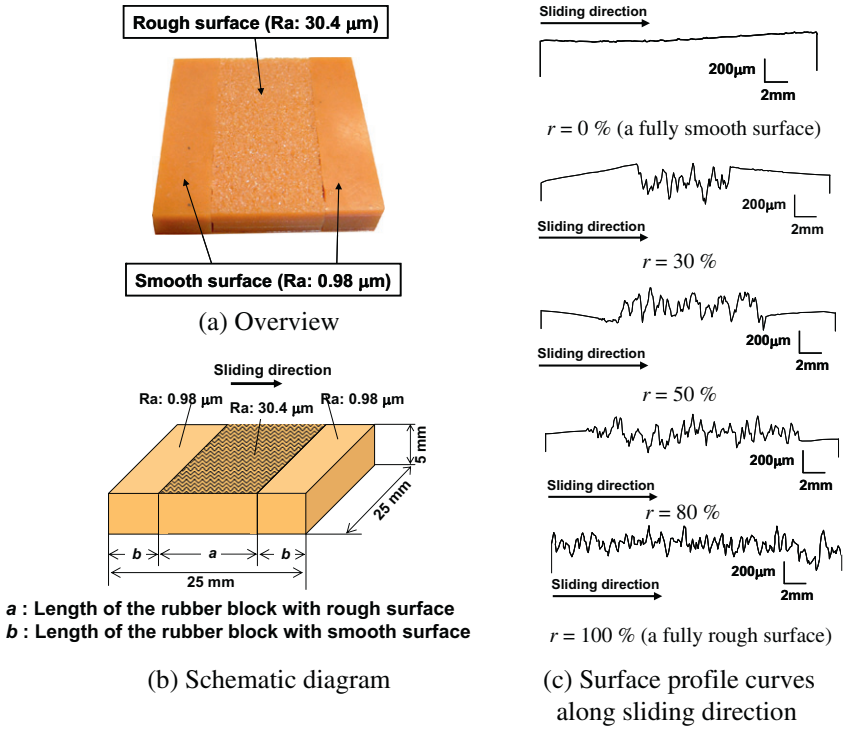


**Fig. 1.** The hybrid rubber blocks with different rough surface area ratios.

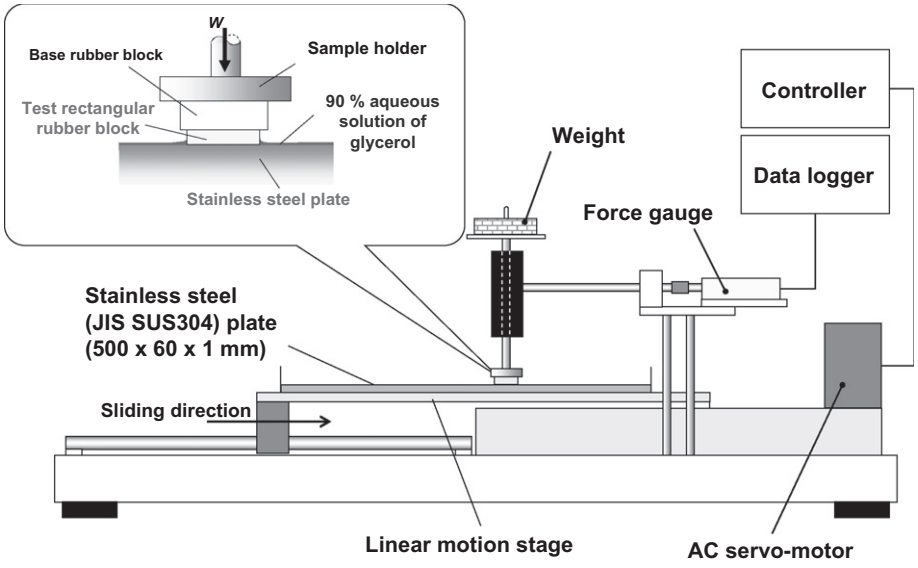


**Fig. 2.** Schematic diagram of the experimental setup for the friction tests using the stainless steel plate.

*2.2.2. Friction test sliding against a polished glass plate*

The rubber block was slid against a polished glass plate (300 mm × 100 mm × 25 mm) with surface roughness Ra of 0.004 μm mounted on the linear motion stage. A LED light was used to illuminate the contact interface between the rubber block and the glass plate, and the contact interface was observed with the high-speed camera through a mirror mounted beneath the glass plate. A normal load was applied by a dead weight. Friction force was measured with a push–pull type force gauge, and the friction force data were recorded by a digital data logger.

The contact area between the rubber block surface and the glass plate surface was measured using the total reflection of light at the contact interface (Childs and Cowburn, 1984). The total internal reflection can occur at the interface between the glass plate and the rubber block or at the interface between the glass plate and the glycerol solution when the angle of incidence $\theta$ is larger than the critical angle $\theta_c$ of each contact interface. The critical angle of incidence $\theta_c$ is determined by the refraction index of each material. The refraction index $n$ values of the NBR, the 90% aqueous solution of glycerol, and the glass plate were 1.52, 1.39, and 1.76, respectively. The total reflection can only occur at the contact interface between the glycerol solution and the glass plate when the angle of incidence is set between 52° and 60°. At these angles of incidence, the contact interface of the rubber block and the glass plate can be observed as a bright section, while the area where the glycerol solution exists between the rubber and the glass will appear as

a dark section due to total reflection between the glass and the glycerol solution. Gray-level photographs taken by the high-speed camera were converted to black-and-white binary images. Then, the contact area ratio $\alpha$, was calculated as the ratio of the contact area between the rubber block and the glass plate (the white section after the conversion) to the apparent contact area (the area of the rubber block surface: 625 $mm^2$. Calculation of the friction coefficient, the definition of the SCOF and the steady-state DCOF in this friction test were the same as those for the friction test on the polished stainless steel plate.

### 2.3. Experimental conditions

The normal load was 56.6 N which included the load of the weight (50 N) and the shaft (6.6 N). The apparent contact pressure between the rubber block and the stainless steel or the glass plate was 90.5 kPa. The contact pressure between the shoe and the floor when a slip event occurs at heel-strike (approximately 410 kPa investigated by Harper et al. (1961)) is much higher than that in this study (approximately 90 kPa). Chang et al. (2001b) indicated that the normal contact pressure should be between 200 and 1000 kPa when the friction force of the shoe/floor contact is measured based on biomechanical observations during normal walking, which is also higher than the normal contact pressure in this study. However, the contact pressures selected as test conditions for field-based friction devices, for measurement of static or steady-state dynamic friction coefficient, ranges from 9 kPa to 400 kPa (Chang et al., 2001c), and the normal contact pressure condition in this study is consistent with this range. 90 wt% aqueous solution of glycerol (viscosity $\eta$: 0.224 Pa. s) was used as a lubricant. Sliding velocity (steady-state linear stage velocity) was 0.2 m/s. These sliding velocity and lubrication conditions were set based on the conditions of the evaluation test of slip-resistance for safety footwear in JIS T8101:2006 (Nagata, 2008). Chang et al. (2001b) suggested the sliding velocity is between zero to 1.0 m/s from a biomechanical analysis of normal walking, and the sliding velocity in this study is within this range. Stage movement was 0.38 m for the friction test using the stainless steel plate or 0.20 m for that using the glass plate. Each rubber block was tested five times under the same conditions. The sampling frequency of the friction force data was 2 kHz, and the data were filtered with a low pass filter using the Butterworth digital filter method. The cut-off frequency was 50 Hz. The frame rate of the high-speed camera was 100 Hz.

## 3. Results and discussion

### 3.1. Effect of the rough surface area ratio on the static and dynamic coefficients of friction of the rubber blocks on the smooth stainless steel plate contaminated with glycerol solution

Fig. 3 shows the variation of the coefficient of friction with time for the rectangular rubber block with different rough surface area ratios. For the rubber block with a fully smooth surface, as shown in Fig. 3a, the coefficient of friction at slip initiation (SCOF) was a small value around 0.1. During the stage acceleration period after the slip was induced, the DCOF increased with time and reached around 1.4, then slightly decreased and resulted in a steady state value greater than 1.0. These results clearly indicate that, for the rectangular rubber block with a fully smooth surface, the SCOF value was significantly smaller than the steady-state DCOF value. On the other hand, for the rubber block with a fully rough surface as shown in Fig. 3b, the SCOF had a high value of around 0.9, then, the coefficient of friction rapidly decreased. During the stage acceleration period after the slip was induced, the DCOF fluctuated due to stick slip. Then, the steady-state DCOF attained a stable low value of less than 0.2. These results show that, for the rubber block with a fully rough surface, the SCOF value was significantly higher than the steady-state DCOF value in contradiction to the case for the rubber block with a fully smooth surface.

On the basis of the results, the SCOF and DCOF values can be controlled with the surface roughness of the rubber block, and a rubber block showing sufficiently high SCOF and DCOF can be realized by combining the rough surface and smooth surfaces.

For other engineering materials such as metallic materials and ceramics which are significantly harder and stiffer than rubbers, increased surface roughness inhibits the formation of a fluid film, by the hydrodynamic lubrication effect, due to surface asperities in the contact area. The lubrication mode of the boundary regime is maintained and a fluid film cannot be easily formed as compared with rubbers. As a consequence, the friction coefficients of these materials with rough surface are higher than rubbers when sliding against surfaces contaminated with a viscous liquid such as the glycerol solution. On the contrary, the hydrodynamic lubrication effect becomes more significant when surface roughness reduces for metallic materials and ceramics.

The SCOF value was smaller than the steady-state DCOF value for the hybrid rubber block with $r = 30\%$ (Fig. 3c). For the hybrid rubber block with $r = 80\%$ (Fig. 3e), the SCOF value was much higher than the steady-state DCOF value. On the other hand, the hybrid rubber block with $r = 50\%$ provided almost the same values of the SCOF and steady-state DCOF, at around 0.5 (Fig. 3d).

The effect of the rough surface area ratio of the hybrid rubber block on the values of SCOF and steady-state DCOF are summarized in Fig. 4. The plot is a mean value, and the error bars are the standard deviation among five experimental results for each rubber block. It can be seen that the SCOF value increased with an increase of rough surface area ratio (Fig. 4a). A bivariate regression analysis between $r$ and the SCOF value indicated that they had a statistically significant relationship ($p < 0.01$) with an extremely high $R^2$ value of 0.99. The steady-state DCOF value linearly decreased with an increase of the rough surface area ratio (Fig. 4b). Therefore, the steady-state DCOF value linearly increased with an increase of the smooth surface area ratio. In addition, a bivariate regression analysis between $r$ and the value of the steady-state DCOF indicated that they had a statistically significant relationship ($p < 0.01$) with extremely high $R^2$ value of 0.96.

Fig. 5 shows the relationship between the values of the SCOF and the steady-state DCOF for each rubber block. The error bars represent the standard deviation. The rough surface area ratio of 50% achieves a relatively high SCOF value of around 0.5 and a relatively high steady-state DCOF value of greater than 0.5. Furthermore, the rubber block with the rough surface area ratio of 50% provided the smallest difference between the SCOF and the steady-state DCOF. Thus, the frictional properties obtained by a rectangular rubber block with a rough surface area ratio of 50% will be effective in preventing slip occurrence and falling due to an induced slip, compared with other rubber blocks, and will be applicable to a high slip-resistant sole pattern for footwear on contaminated surfaces.

### 3.2. Effect of the contact area between the rubber block and the smooth glass plate on the static and dynamic coefficients of friction

In this section, the direct contact area between the rubber and the glass during sliding was measured using the total reflection of light. The mechanism for high values of the SCOF and the DCOF obtained from the hybrid rectangular rubber block was suggested from the viewpoint of the contact area.

Fig. 6a shows the coefficient of friction as a function of time for the rubber block with a fully smooth surface ($r = 0\%$) and sequen-

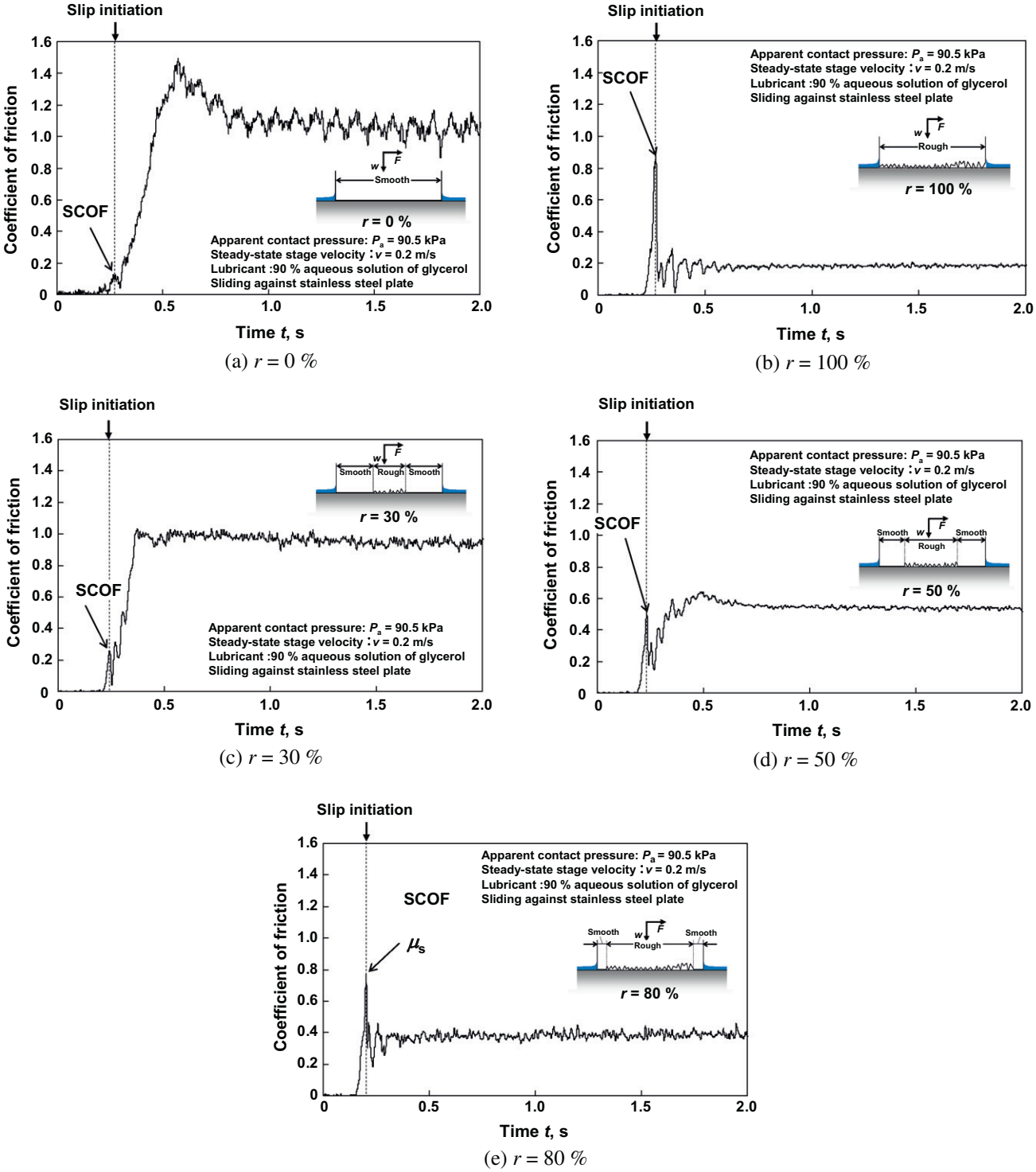


**Fig. 3.** Variation of the coefficient of friction with time for the rubber blocks.

tial snapshots of the binary images of the contact interface between the rubber block and the glass plate contaminated with 90% aqueous solution of glycerol. At the slip initiation, the contact area between the rubber block and the glass plate (white area) was negligible and the SCOF value was very small because the glycerol solution film existed in the contact interface. Then, the coefficient of friction increases as the contact area increases. Eventually at the steady-state sliding, an anterior half part of the rubber block directly contacted with the glass plate and the steady-stale DCOF took high value around 1.0. Fig. 6b shows the coefficient of friction as a function of time for the rubber block with a fully rough surface ($r$ = 100%) and sequential snapshots of the binary images of the contact interface between the rubber block and the glass plate. The asperities of the rough rubber surface directly contacted with the glass plate both at the slip initiation and the steady-state sliding. The contact area at the slip initiation is clearly higher than that of the rubber block with a fully smooth surface. However, the contact area at the steady-state sliding is smaller than that of the rubber block with a fully smooth surface. Fig. 6c shows the coefficient of friction as a function of time for the hybrid rectangular rubber

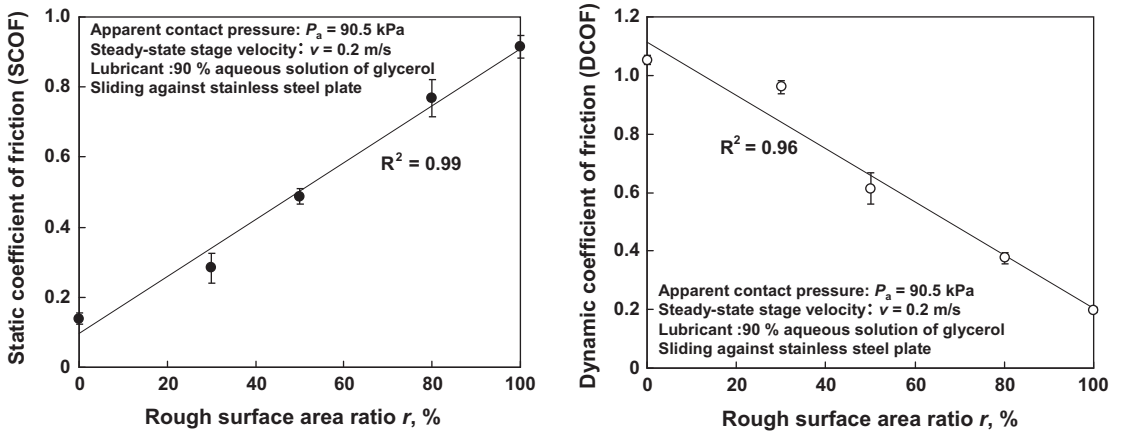


(a) Static coefficient of friction (b) Steady-state dynamic coefficient of friction

**Fig. 4.** Effect of the rough surface area ratio of the rubber block surfaces on the static and steady-state dynamic coefficients of friction.

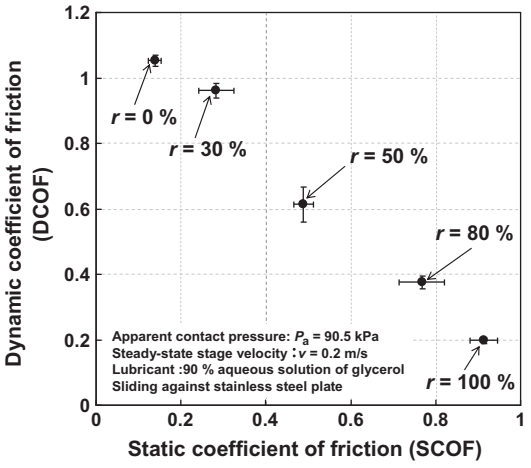


**Fig. 5.** Relationship between the static coefficient of friction and the steady-state dynamic coefficient of friction for each rubber block.

block combining smooth and rough surfaces ($r$ = 50%) and sequential snapshots of the binary images of the contact interface between the rubber block and the glass plate. Only the asperities of the rough rubber surface directly contacted with the glass plate at slip initiation, which resulted in high SCOF values. It can also be seen in Fig. 6c that the smooth rubber surface located anteriorly contacted directly with the glass plate in addition to the asperities of the rough rubber surface during steady-state sliding.

The relationship between the SCOF value and the contact area ratio $\alpha_s$ at slip initiation is shown in Fig. 7a. The SCOF value increased with an increase of contact area ratio $\alpha_s$, and a higher rough surface area ratio had a tendency to increase contact area ratio at the slip initiation. The relationship between the DCOF value and the contact area ratio $\alpha_d$ during steady-state sliding is shown in Fig. 7b. The steady state DCOF value also increased with an increase in the contact area ratio. In addition, the lower rough surface area ratio had a tendency to provide a higher contact area ratio during steady-state sliding. These results indicate that the rubber block combining rough and smooth surfaces, the contribution of the two surface-types maintains the direct contact between the rubber and the glass plate, both at the slip initiation and during steady-state sliding. Consequently, this mechanism can provide high values of SCOF and DCOF.

### *3.3. Mechanism of high static and dynamic friction for the hybrid rubber block combining rough and smooth surfaces*

The contact area measurements between the rubber block and the glass plate are indicative of the friction mechanisms of each rectangular rubber block as shown in Fig. 8.

For the rubber block with a fully smooth surface, a thin film of glycerol solution remains in the contact interface due to the low contact pressure at the slip initiation. Thus, the static friction force is determined by the low shear strength of the glycerol solution film. On the other hand during steady-state sliding, the anterior right edge of the rubber block can prevent infiltration of the glycerol solution into the contact interface, which allows for the direct contact of the anterior part of the smooth rubber surface with the stainless steel surface. Thus, the steady-state DCOF reached a sufficiently high value greater than 1.0. For the rubber block with a fully rough surface, the glycerol solution film is removed at slip initiation by the high contact pressure due to the rough surface asperities; this effect results in direct contact between the asperities of the rough rubber surface and the stainless steel. Thus, the SCOF achieves a high value. On the other hand during steady-state sliding, the anterior edge of the rubber block cannot prevent infiltration of the glycerol solution into the contact interface, due to the large surface roughness. The lubrication mode would be boundary or mixed lubrication during steady-state sliding period. Thus, the steady-state DCOF attained low value of 0.2 or less.

For the hybrid rubber block with $r$ = 50%, the rough surface component would prevent film formation due to the high contact pressure and would realize direct contact between asperities of the rubber surface and the stainless steel; however, the smooth surface component would not contribute to the increase of direct contact area because a thin film of glycerol solution remains at slip initiation. Therefore, the SCOF achieved relatively high value but these were less than those for the rubber block with a fully rough surface ($r$ = 100%). During the steady-state sliding period, the anterior right edge of the smooth surface component prevents infiltration of the glycerol solution into the contact interface, which allows direct contact between the smooth rubber surface and the stainless steel surface. However, the contact area of the smooth surface and the stainless steel is determined by the rough surface area ratio; therefore, the steady-state DCOF achieved relatively high value but these were less than those for the rubber block with a fully smooth surface ($r$ = 0%).

The surface roughness of the stainless steel plate used for friction measurement and that of the glass plate used for contact area

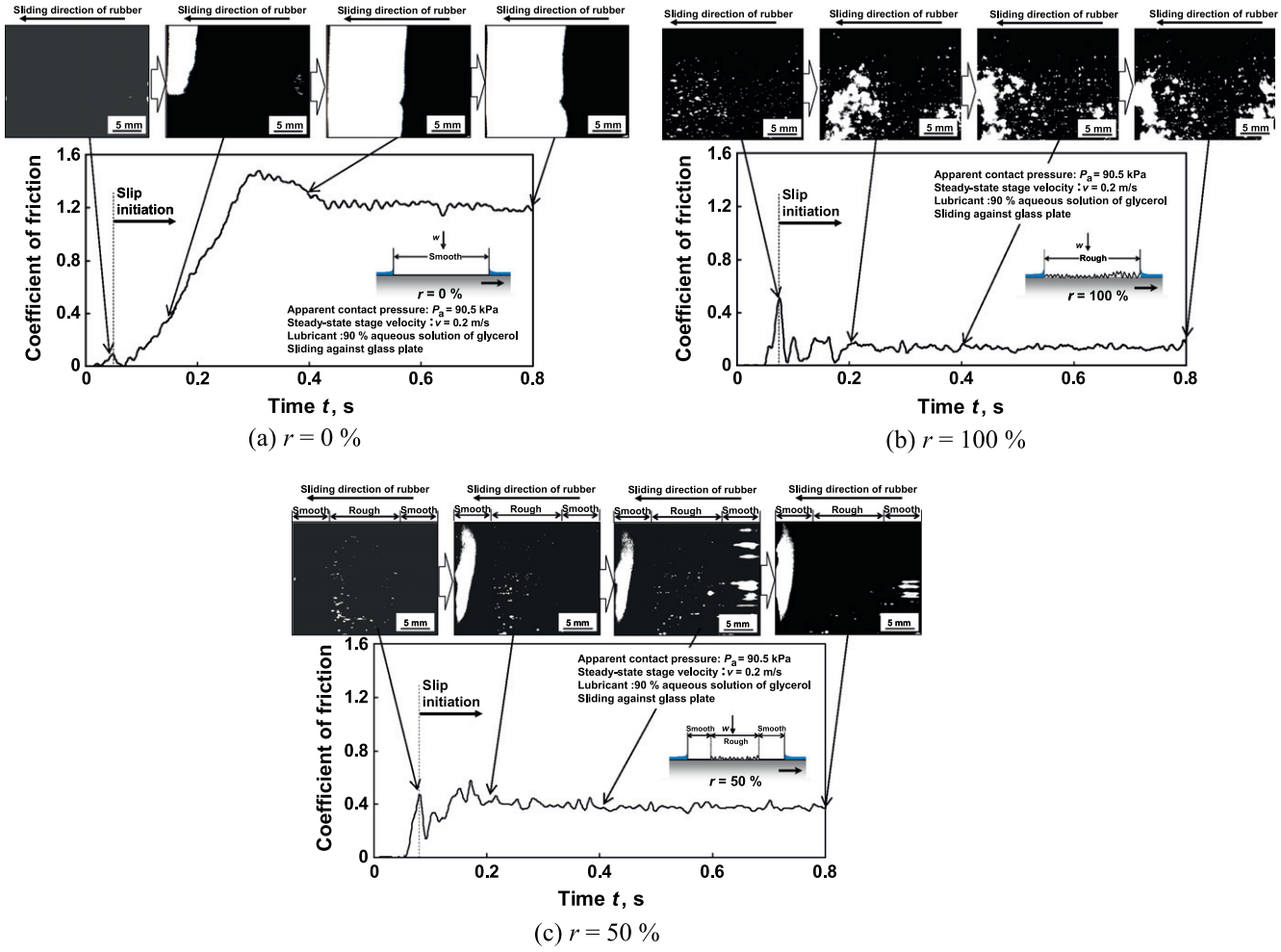


**Fig. 6.** Coefficient of friction as a function of time and sequential snapshots of the black-and-white binary images of the contact interface between the rubber block and the glass plate. White section in the binary image corresponds to contact area between rubber and glass plate.

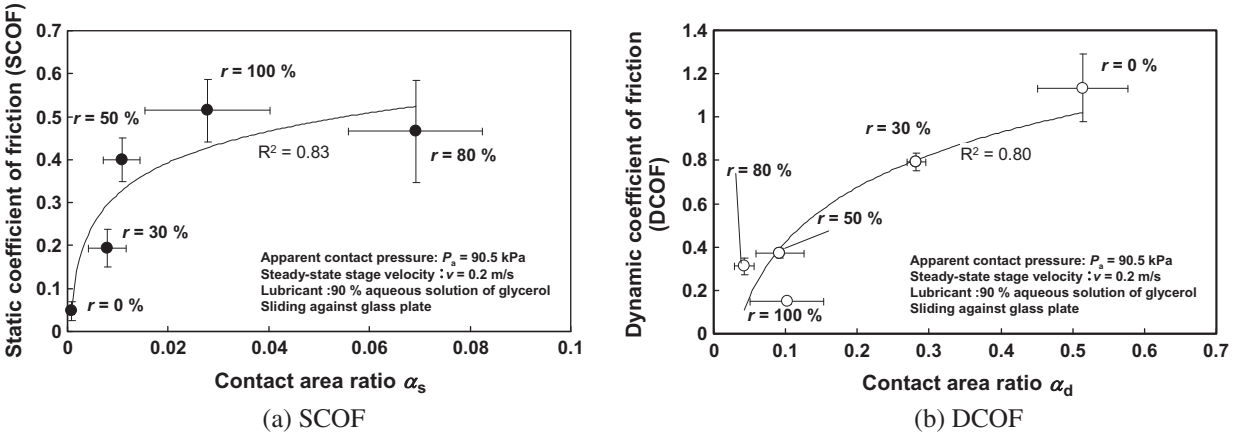


**Fig. 7.** The relationship between the coefficients of friction and the contact area ratio.

measurements was different. It is well known that friction and contact phenomena are affected by surface roughness. The stainless steel plate and glass plate surfaces were mirror-polished and the surface roughness for each was below 0.1 μm Ra, which would be small enough not to affect the results of the SCOF and DCOF measurement. From Figs. 4 and 7, it can be seen that the effect of rough surface area ratio on the SCOF and DCOF; the SCOF increases with an increase of the rough surface area ratio and the DCOF decreases with an increase of the rough surface area ratio, was almost the same for the two surface types. The range of values of the SCOF and DCOF for the stainless steel plate tests and those for the glass plate tests were not so significantly different. Thus, the friction phenomena at the contact interface would be identical for rubber/stainless steel and rubber/glass. Consequently, the mecha-

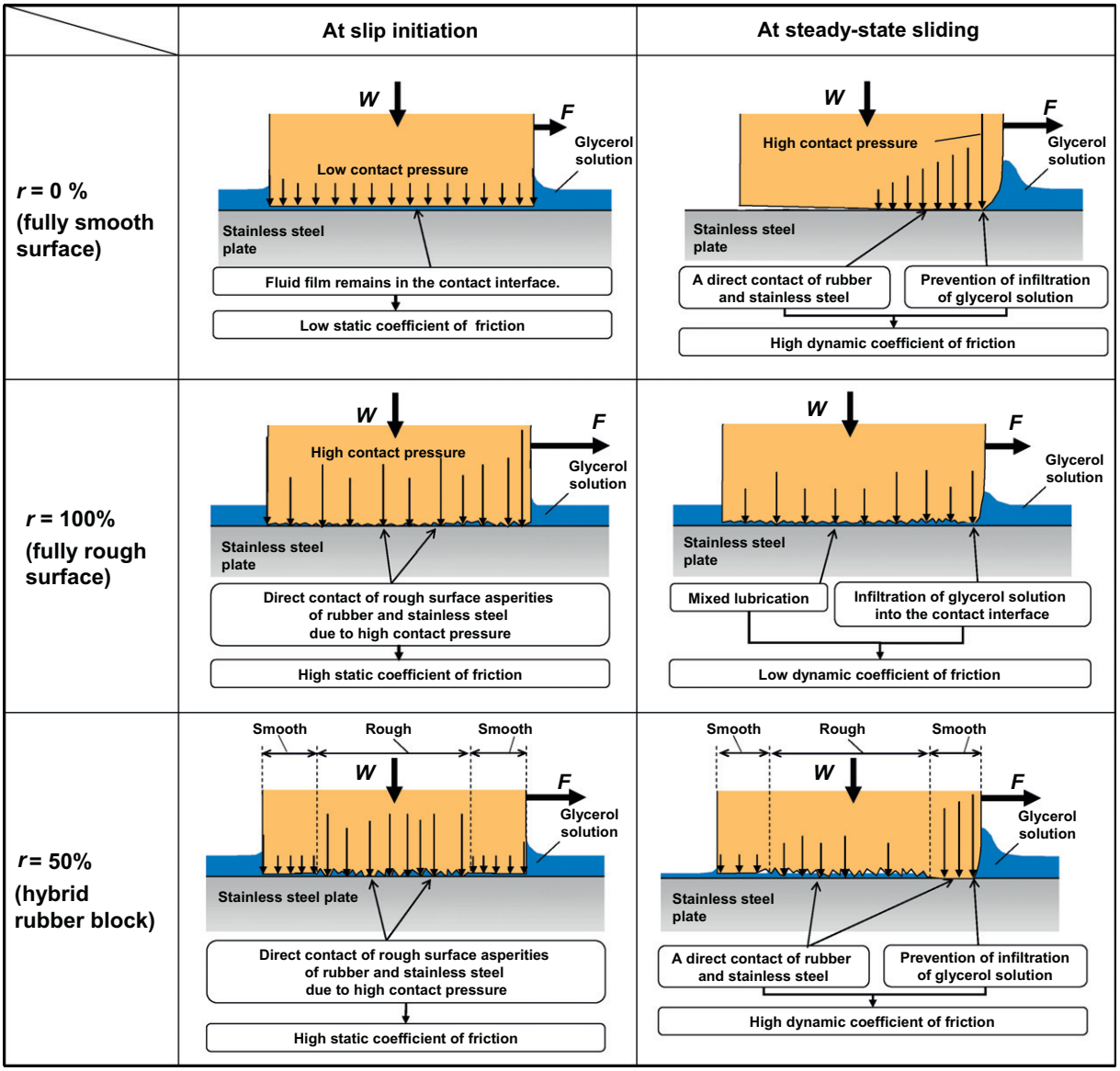


**Fig. 8.** Schematic diagram of the contact interface between the rubber blocks with $r$ values of 0%, 50%, 100% and the stainless steel plate contaminated with the glycerol solution.

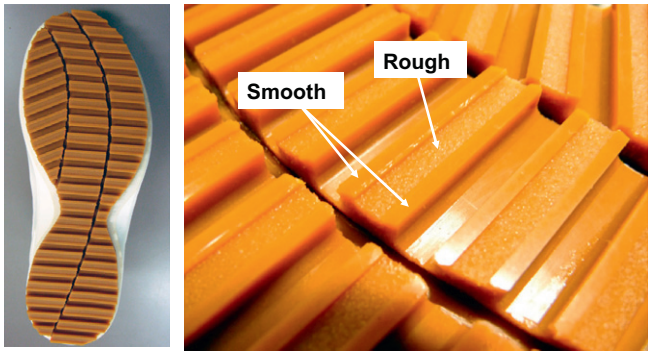


**Fig. 9.** The shoe sole pattern by use of the hybrid rubber block ($r$ = 50%).

nisms derived from the contact area measurements obtained from the glass plate tests would be applicable to the rubber block/stainless steel plate conditions.

Based on the results obtained in this study, a footwear sole pattern utilizing hybrid rubber blocks combining smooth and rough surfaces ($r$ = 50%) was prepared as shown in Fig. 9. Further investigations are needed to investigate the effectiveness and practicality of this sole pattern through gait experiments on a contaminated smooth surface.

The results obtained in this study provide an example of the design guidelines for a shoe sole pattern with high slip resistance; i.e. both sufficiently high static and dynamic coefficients of friction, on contaminated surfaces based on tribological approaches including friction and contact area measurements. This study will lead to a reduction in the risk of slip and fall accidents in the workplace with liquid contaminated floors.

## 4. Conclusions

In order to prevent slip initiation during walking, sufficient static friction is needed in the contact interface between the footwear sole and the floor. Sufficiently high dynamic friction is also re-

quired to help postural recovery after slipping. In this study, a new footwear sole surface pattern was developed to increase the static friction and the dynamic friction when sliding against a liquid-contaminated surface. Hybrid rubber blocks, in which a rubber block with a rough surface (Ra = 30.4 μm) was sandwiched between two rubber blocks with a smooth surface (Ra = 0.98 μm), were prepared. The rough surface area ratio $r$ was 0%, 30%, 50%, 80%, and 100%. Friction tests were conducted using a reciprocating linear sliding type tribo-meter. The rubber block was slid against a stainless steel (JIS SUS304) plate with Ra of 0.09 μm, contaminated with 90% aqueous solution of glycerol. The SCOF and the steady-state DCOF values of the hybrid rubber blocks were affected by the rough surface area ratio $r$. The SCOF value increased with an increase of the rough surface area ratio $r$ while the steady-state DCOF value decreased with an increase of the rough surface area ratio $r$. A rough surface area ratio of 50% achieved high SCOF values of around 0.5 and high steady-state DCOF values greater than 0.5. Furthermore, the difference in these values was the smallest for the hybrid rubber block with $r$ = 50%. Thus, it can be considered the rubber block with $r$ = 50% is applicable to the footwear sole pattern with high-slip resistance.

Through the observation of the contact interface using the total reflection of light method, the contact area between the rubber and the glass contaminated with a glycerol solution was measured. An analysis of the contact area ratio between the rubber block and the glass plate revealed that high values of the SCOF and the steady-state DCOF for the hybrid rubber blocks were realized by maintaining direct contact between the rubber and the mating surfaces both at slip initiation and during steady-state sliding.

## Acknowledgment

The authors would like to thank Dr. Hisao Nagata for valuable comments and suggestions that have strengthened this paper.

## References

Bowen, F.P., Tabor, D., 1950. The Friction and Lubrication of Solids. Clarendon Press, Oxford.

Chang, W.R., Kim, I.J., Manning, D.P., Bunterngchit, Y., 2001a. The role of surface roughness in the measurement of slipperiness. Ergonomics 44, 1200–1216.

Chang, W.R., Grönqvist, R., Lecrercq, S., Myung, R., Makkonen, L., Strandberg, L., Brungraber, R.J., Mattke, U., Thorpe, S.C., 2001b. The role of friction in the measurement of slipperiness, Part 1: friction mechanism and definition of test conditions. Ergonomics 44, 1217–1232.

Chang, W.R., Grönqvist, R., Lecrercq, S., Brungraber, R.J., Mattke, U., Strandberg, L., Thorpe, S.C., Myung, R., Makkonen, L., Courtney, T.K., 2001c. The role of friction in the measurement of slipperiness, Part 2: survey of friction measurement devices. Ergonomics 44, 1233–1261.

Childs, T.H.C., Cowburn, D., 1984. Contact observations on and friction of rubber drive belting. Wear 100, 59–76.

Courtney, T.K., Webster, B., 2001. Antecedent factors and disabling occupational morbidity – insights from the new BLS data. American Industrial Hygiene Association Journal 62, 622–632.

Courtney, T.K., Sorock, G.S., Manning, D.P., Collins, J.W., Holbein-Jenny, M.A., 2001. Occupational slip, trip, and fall-related injuries – can the contribution of slipperiness be isolated? Ergonomics 44, 1118–1137.

Ekkubus, C.F., Killey, W., 1973. Validity of 0.5 static coefficient of friction (James Machine) as a measure of safe walkway surfaces. Soap/Cosmetics/Chemical Specialties 49 (2), 40–45.

Fong, D.T.P., Hong, Y., Li, J.X., 2009. Human walks carefully when the ground dynamic coefficient of friction drops below 0.41. Safety Science 47, 1429–1433.

Grönqvist, R., 1995. Mechanisms of friction and assessment of slip resistance of new and used footwear soles on contaminated floors. Ergonomics 38, 224–241.

Grönqvist, R., Roine, J., Järvinen, E., Korhonen, E., 1989. An apparatus and a method for determining the slip resistance of shoes and floors by simulation of human foot motions. Ergonomics 32 (8), 979–995.

Grönqvist, R., Hirvonen, M., Tohv, A., 1999. Evaluation of three portable floor slipperiness testers. International Journal of Industrial Ergonomics 25, 85–95.

Grönqvist, R., Hirvonen, M., Rajamaki, E., Matz, S., 2003. The validity and reliability of a portable slip meter for determining floor slipperiness during simulated heel strike. Accident Analysis and Prevention 35 (2), 211–225.

Harper, F.C., Warlow, W.J., Clarke, B.L., 1961. The Forces Applied to the Floor by the Foot in Walking, National Building Research Paper 32, DSIR, Building Research Station. HMSO, London.

James, D.I., 1990. Assessing the slip resistance of flooring materials. In: Gray, B.E. (Ed.), Slips, Stumbles, and Falls: Pedestrian Footwear and Surfaces. ASTM, Philadelphia, PA, pp. 133–144.

Leclercq, S., Tisserand, M., Saulnier, H., 1995. Tribological concepts involved in slipping accidents analysis. Ergonomics 38 (2), 197–208.

Li, K.W., Chen, C.J., 2004. The effect of footwear soling tread groove width on the coefficient of friction with different sole materials, floors, and contaminants. Applied Ergonomics 35, 499–507.

Li, K.W., Chen, C.J., 2005. Effects of tread groove orientation and width of the footwear pads on measured friction coefficients. Safety Science 43, 391–405.

Manning, D.P., Jones, C., 2001. The effect of roughness, floor polish, water, oil and ice on underfoot friction: current safety footwear solings are less slip resistant than microcellular polyurethane. Applied Ergonomics 32, 185–196.

Minister's Secretariat Statistics and Information Department of Ministry of Health, Labour and Welfare, 2006. Vital Statistics of Japan 2004, vol. 1. Health & Welfare Statistics Association.

Nagata, H., 2008. Test methods for slip resistance and Japanese industrial standards of protective footwear. Journal of Japanese Society of Tribologists 53 (8), 524–529.

Nagata, H., Watanabe, H., Inoue, Y., Kim, I.J., 2009. Fall and validities of various methods to measure frictional properties of slippery floors covered with soapsuds. In: Proceedings of the 17th World Congress on Ergonomics, Beijing.

Perkins, P.J., 1978. Measurement of slip between the footwear and ground during walking. In: Anderson, C., Senne, J. (Eds.), Walkway surfaces: measurement of slip resistance, ASTM STP 649. American Society for Testing and Materials, Philadelphia, PA, pp. 71–87.

Perkins, P.J., Wilson, M.P., 1983. Slip resistance of testing footwears – new developments. Ergonomics 26, 73–82.

Pilla, D.S., 2003. Slip and Fall Prevention: A Practical Handbook. Lewis Publishers, USA.

Poon, C.Y., Bhushan, B., 1995. Comparison of surface roughness measurements by stylus profiler, AFM and non-contact optical profiler. Wear 190, 76–88.

Proctor, T.D., Coleman, V., 1988. Slipping, tripping, and falling accidents in Great Britain – present and future. Journal of Occupational Accidents 9, 269–285.

Redfern, M.S., Bidanda, B., 1994. Slip resistance of the shoe–floor interface under biomechanically-relevant conditions. Ergonomics 37 (3), 511–524.

Strandberg, L., 1983. On accident analysis and slip-resistance measurement. Ergonomics 26, 11–32.

Strandberg, L., 1985. The effect of conditions underfoot on falling and overexertion accidents. Ergonomics 28 (1), 131–147.

Strandberg, L., Lanshammar, H., 1981. The dynamics of slipping accidents. Journal of Occupational Accidents 3, 153–162.

Tisserand, M., 1985. Progress in the prevention of falls caused by slipping. Ergonomics 28, 1027–1042.

Wilson, M., 1990. Development of SATRA slip test and tread pattern design guidelines. In: Gray, B.E. (Ed.), Slips, Stumbles, and Falls: Pedestrian Footwear and Surfaces, ASTM STP 1103. American Society for Testing and Materials, Philadelphia, pp. 113–123.

Yamaguchi, T., Hokkirigawa, K., 2008. 'Walking-Mode Maps' based on slip/non-slip criteria. Industrial Health 46, 23–31.